HHS Public Access

Author manuscript

Ann Biomed Eng. Author manuscript; available in PMC 2017 June 12.

Published in final edited form as:

Ann Biomed Eng. 2011 June ; 39(6): 1654–1667. doi:10.1007/s10439-011-0273-x.

The Effects of Combined Cyclic Stretch and Pressure on the Aortic Valve Interstitial Cell Phenotype

Patrick Thayer[1], **Kartik Balachandran**[1], **Swetha Rathan**[2], **Choon Hwai Yap**[1], **Sivakkumar Arjunon**[1], **Hanjoong Jo**[3], and **Ajit P. Yoganathan**[1]

[1]W.H. Coulter School of Biomedical Engineering, Georgia Institute of Technology, Atlanta, GA, USA

[2]School of Chemical and Biomolecular Engineering, Georgia Institute of Technology, Atlanta, GA, USA

[3]Department of Cardiology, Emory University, Atlanta, GA, USA

Abstract

Aortic valve interstitial cells (VIC) can exhibit phenotypic characteristics of fibroblasts, myofibroblasts, and smooth muscle cells. Others have proposed that valve cells become activated and exhibit myofibroblast or fibroblast characteristics during disease initiation and progression; however, the cues that modulate this phenotypic change remain unclear. We hypothesize that the mechanical forces experienced by the valve play a role in regulating the native phenotype of the valve and that altered mechanical forces result in an activated phenotype. Using a novel *ex vivo* cyclic stretch and pressure bioreactor, we subjected porcine aortic valve (AV) leaflets to combinations of normal and pathological stretch and pressure magnitudes. The myofibroblast markers α-SMA and Vimentin, along with the smooth muscle markers Calponin and Caldesmon, were analyzed using immunohistochemistry and immunoblotting. Tissue structure was analyzed using Movat's pentachrome staining. We report that pathological stretch and pressure inhibited the contractile and possibly myofibroblast phenotypes as indicated by downregulation of the proteins α-SMA, Vimentin, and Calponin. In particular, Calponin downregulation implies depolymerization of actin filaments and possible conversion to a more synthetic (non-contractile) phenotype. This agreed well with the increase in spongiosa and fibrosa thickness observed under elevated pressure and stretch that are typically indicative of increased matrix synthesis. Our study therefore demonstrates how cyclic stretch and pressure may possibly act together to modulate the AVIC phenotype.

Keywords

Aortic valve; Stretch; Pressure; Phenotype

Address correspondence to Ajit P. Yoganathan, W.H. Coulter School of Biomedical Engineering, Georgia Institute of Technology, Atlanta, GA, USA. ajit.yoganathan@bme.gatech.edu.

Associate Editor Jane Grande-Allen oversaw the review of this article.

INTRODUCTION

The aortic valve (AV) is an elegant and sophisticated structure that is exposed to a multitude of forces during its approximate 100,000 cycles a day for a life time.[19] The cusps of AV withstand great stress and deformation during a cardiac cycle. The underlying extracellular structure of the leaflet gives the valve the ability to maintain its integrity. Normal hemodynamic forces, consisting of tension, compression, and shear forces at various stages of the cardiac cycle, have been shown to result in the maintenance of the valvular biological phenotype[14,25] of AV. These mechanical forces are also known to induce changes within the cellular architecture.[11] The mechanobiological response of the cells to pathophysiological forces has been correlated with remodeling of the valve leaflets, leading to disease.[2,3] However, the exact mechanisms for these responses are still not well understood.

Of particular interest in our laboratory is the modulation of the valve cell phenotype in response to mechanical stimulation. Taylor *et al.* reported that the valve interstitial cells (VIC) can exist as non-contractile or contractile phenotypes, with an intermediate state comprised of activated myofibroblasts that stain positive for α-smooth muscle cell actin (α-SMA).[28] Several researchers have correlated this activated state of the valve cell to eventual diseased states.[15,24] In our laboratory, we demonstrated that exposing AV leaflets to isolated cyclic stretch results in an upregulation of α-SMA.[1] Isolated pressure was shown to downregulate α-SMA expression compared to fresh tissue regardless of pressure magnitude.[30] It has been speculated that various mechanical forces regulate the contractile and synthetic phenotypes of the aortic VICs. It is suspected that pathological hemodynamic environments may shift the equilibrium of cell phenotypes and may play a role in AV disease.

Vimentin is another cytoskeletal component that provides stiffness; it is expressed abundantly in fibroblasts and endothelial cells.[29] Vimentin expression has been shown to have a much greater expression in the left ventricle endothelium compared to the right, perhaps because of increased blood pressure.[26] In addition, the native expression of Vimentin in the ventricularis side of the AV is higher than the pulmonary valve, further supporting the evidence that Vimentin is expressed more in high pressure areas.[5] Two other proteins of interest are Caldesmon and Calponin, which are expressed in smooth muscle cells and bind to Actin and Calmodulin.[20] It is theorized that Caldesmon is restricted to the contractile apparatus of the smooth muscle cells; binding to Actin.[16] Calponin serves a similar function and it is involved in cytoskeletal Actin binding and bundling. It is also an indicator for contractile phenotype of the cells.[7] More specifically, Calponin has been shown to be regulated as a result of mechanical tension in various types of cells.[10] These three mechanosensitive cytoskeletal proteins have not been studied well in the context of valve mechanobiology, especially to understand whether an altered mechanical environment affects their expression in AV cells. Further, Caldesmon and Calponin are related to the formation and function of Smooth Muscle Actin, and it is worth comparing their expression display trends to that of α-SMA.

Studies to date have focused primarily on the effect of a single mechanical force on valve biology.[3,27,31] It is unclear how a combination of mechanical forces will modulate cell

phenotype. We hypothesize that the combination of the two forces will result in an additive or synergistic effect in modulating valve cell phenotype. We designed and fabricated a novel *ex vivo* stretch-pressure bioreactor, and utilized this device to show that combined elevated stretch and pressure result in a downregulation of the contractile phenotype in aortic VICs, showing opposing mechanostimulatory roles between pressure and stretch.

MATERIALS AND METHODS

Tissue Harvest

Fresh porcine (female, healthy, non-pregnant, aged 6–12 months) AVs were obtained from a local abattoir (Holifield Farms, Covington, GA) following on-site dissection of the hearts within 30 min of slaughter. The valves were then transported to the laboratory in sterile, Dulbecco's Phosphate Buffered Saline (dPBS; Sigma, St. Louis, MO) on ice. Upon arrival to the laboratory, a rectangular section of 15 by 5 mm was isolated from the center of each leaflet (Fig. 1a). This tissue sample was oriented in the circumferential direction from the basal region. The samples were randomly assigned to stretch and combined stretch-pressure groups. The leaflet sections then had springs threaded through the 5 mm ends (Fig. 1b) and were suspended in Dulbecco's Modified Eagle Medium (DMEM) in a custom stretch-pressure bioreactor (Figs. 1c, 1d, and 1f). These samples were then cyclically stretched at a frequency of 1.167 Hz (equivalent to 70 beats per minute) at 10% or 15% stretch at 37 °C for 48 h. The leaflet sections from the combined stretch and pressure group were simultaneously exposed to the same tensile waveform as the stretch-only samples. A cyclic pressure of either 120/80 mmHg (normal) or 140/100 mmHg (pathologic/hypertensive) was applied. This cyclic pressure was synchronized to be out of phase with the cyclic stretch as the maximum stretch occurred during diastole when the aortic pressure is at its minimum (Fig. 2).

Stretch-Pressure Bioreactor System and Validation

The base stretch bioreactor used in this study was similar to the one used previously in our lab.[1,3] The base stretch bioreactor was comprised of two chambers with eight wells in each. The two chambers were connected externally via a movable arm which was controlled by a linear actuator that stretched the samples uniformly. This bioreactor design has been validated previously.[1,2] The base stretch bioreactor was modified in such a way to allow for the application of a cyclic pressure to the samples. A pressure chamber was added as a lid to one of the stretch chambers. The top of the chamber contained a nozzle for attaching a hose attachment. A double-layered neoprene membrane was used as a deflection membrane for transmitting the pressure to the stretch chambers. The membranes were held in place using 20 stainless steel screws. The pressure chamber was clamped to the stretch chamber via eight screws, creating an airtight seal. The pressure in the bioreactor was constantly monitored with a pressure transducer (Validyne Engineering, Northridge, CA). The pressure transducer was attached to the wells of the stretch chamber via a luer lock connector (McMaster Carr, Cleveland, OH). A hose was attached to the nozzle and on the other end clamped to a solenoid valve. The solenoid valve was used to control the airflow into the pressure chamber from an air compressor. A custom Labview program (Texas Instruments) controls the pressure waveform to the solenoid pump through a DAQ controller. A schematic

of this control is depicted in Fig. 1e. The bioreactor was validated to ensure that the desired pressures and synchrony with stretch was achieved over the entire duration of the experiment.

Since the bioreactor will have high pressure in the tissue chamber constantly, dissolved gases concentrations will increase. To account for this, culture media without tissue samples was exposed to pulsatile pressure peaking at 170 mmHg for 48 h, and dissolved carbon dioxide concentration was measured by measuring the pH of the culture media using a pH meter (Orion Model 310, ThermoFisher Scientific, Waltham, MA). Further, culture media without tissue samples were exposed to pulsatile pressure peaking at 170 mmHg for 24 h and dissolved oxygen concentration was measured with a dissolved oxygen meter (Model 5100, YSI Life Sciences, Yellow Springs, OH).

The bioreactor was sterilized using ethylene oxide gas and assembled aseptically in a sterile laminar flow hood (Fisher Hamilton, Two Rivers, WI). The culture wells were filled with 8 mL of DMEM supplemented with 10% fetal bovine serum, 50 mg/L ascorbic acid, 3.7 g/L sodium bicarbonate, 1% (v/v) non-essential amino acid solution, and 1% (v/v) antimycotic-antibiotic solution (all reagents from Sigma), pH adjusted to 7.4. Each tissue section was suspended in the medium by the two springs—one end was looped around the stationary posts while the other end was looped around the moving post. The bioreactor was then placed in an incubator (Fisher Scientific, Hampton, NH) maintained at 37 °C, 5% CO_2 while being operated for 48 h.

Tissue Processing

At the end of the experiment, each leaflet section was removed; the springs were cut off from the ends of the tissue, and the samples were washed in sterile dPBS. For histological and immunohistochemical analyses, leaflet sections were fixed in 10% neutral buffered formalin (Fisher Scientific, Suwanee, GA) for 24 h, saturated in 70% ethanol, embedded in paraffin and sliced into 5 μm sections for analysis using a microtome and fixed on slides.

Tissue Morphology

Tissue morphology was accessed by staining using a Russell-Movat pentachrome stain kit (American MasterTech Scientific, Lodi, CA). The procedure is as follows: Slides were deparaffinized using xylene, hydrated with alcohols and rinsed with DI water. The slide was placed in the Verhoeff's elastic stain (20 mL of 10% alcoholic hematoxylin, 20 mL of reagent alcohol, 20 mL of 10% ferric chloride, and 20 mL of universal iodine solution) for 15–20 min, followed by rinsing with lukewarm tap water for 5 min and DI water. The section was then differentiated with 2% ferric chloride until the elastic fibers are defined, the slide is then rinsed with DI water and then placed in 5% sodium thiosulfate for 1 min. The slide was then rinsed again in tap water for 5 min and then placed in a 3% glacial acetic acid solution for 3 min. The slide was then placed directly in a 1% alcian blue solution for 15–30 min or until the mucins are blue then rinsed for 1 min in warm tap water and then DI water. The slide was then place in a solution of crocein scarlet-acid fuchsin for 2 min followed by rinsing in three changes of DI water. The slide was then dipped five times in 1% glacial acetic acid. The slide was then placed in two changes of 5% phosphotungstic acid for 2–5

until connective tissue is clear but before the elastin is de-stained. The slide is then dipped five times in 1% glacial acetic acid and rehydrated through three changes of fresh absolute alcohol. The plate was finally placed in alcoholic saffron solution for 15 min and dehydrated through three changes of fresh absolute alcohol, followed by three changes of fresh xylene and then cover slipped. The slides were then imaged at 100 × using a light microscope.

Cell Phenotype

For immunostaining, the slides were de-paraffinized and blocked using 1% bovine serum albumin (BSA)/PBS (Sigma) for 30 min. The slides were then incubated in either mouse monoclonal anti α-SMA, Vimentin, Calponin, or Caldesmon primary antibodies (Sigma) in 1% BSA/PBS (Sigma) for 1 h. The sections were saturated in biotinylated horse anti-mouse IgG (Vector laboratories) in 1% BSA/PBS, and 2% normal horse serum (Vector laboratories) for 30 min. Avidin-D Texas red (Vector laboratories) fluorochrome was applied to the sections after the secondary antibody was washed off. The sections were then counter stained with 0.25 μg/mL 4′,6-diamidino-2-phenylindole (DAPI; Sigma), cover slipped, and stored at 4 °C. Slides were then imaged at 200 × using a TR-FITC-DAPI triple filter under a mercury lamp.

For immunoblotting, equal amounts (30 μg) of tissue lysates were resolved by reducing SDS-polyacrylamide gel electrophoresis. After transfer to a polyvinylidene difluoride membrane (Millipore), the blots were blocked with 5% non-fat dry milk and probed with primary antibody and appropriate biotinylated secondary antibody. Immunoblotting was used to analyze expression of α-SMA (1:100, Sigma), Caldesmon (1:30, Sigma), and β-actin (1:100, Sigma). The membranes were finally incubated in horseradish peroxidase-conjugated streptavidin. Immunopositive bands were detected by using a luminol-based chemiluminescence reagent (Pierce), imaged in a darkroom, and analyzed by densitometry by using the Image J program (NIH).

Image Analysis

For the Movat pentachrome images, the fibrosa: spongiosa length ratio and the ventricularis:fibrosa length ratio were measured at eight different locations per images, using ImageJ© (National Institutes of Health, Bethesda, MD). The ventricularis was defined as the area where the elastin fibers (black) were present with relatively smooth edge. The fibrosa was defined as the area that collagen (yellow) was primarily located with relatively wavy tissue edge. The spongiosa was the area between the ventricularis and fibrosa. For the immunohistological images, proteins (such as α-SMA, Vimentin, Calponin, and Caldesmon) immune-positive cells were made to appear red, while cell nuclei were counterstained blue. The proportion of immune-positive cells were quantified using the ImageJ (National Institutes of Health, Bethesda, MD) to determine the relative coverage area of protein positive red staining compared to the coverage area of the entire leaflet section, normalized by the number of cells. This method has been previously utilized in our laboratory.[1,2,21]

Statistical Analysis

All quantitative data were expressed as mean ± standard error. The sample size was n = 6–8 for the immunostaining analyses, n = 3 for histological stains, and n = 4 for western blots.

Data were first tested for normality using the Anderson-Darling test. Normal data was statistically tested using a one-way ANOVA to determine the effects of the different mechanical treatments on cell phenotype. This was followed by pairwise comparison using the Tukey method. Data that failed the test for normality was tested using a one-way ANOVA on ranks followed by pairwise comparison using the Dunn's *post hoc* test. In addition, we also reported any additional statistical differences between the normal condition (10% 120/80 mmHg) and the hypertensive condition (15% 140/100 mmHg) using Student's *t* test. All immunostaining and immunoblot results were normalized by the 10% stretch case. A p value of less than 0.05 was used as a measure of statistical significance. A trend toward significance when the p value was less than 0.1 has also been indicated. All statistical analyses were performed using JMP (SAS Institute Inc.) software.

RESULTS

Design and Validation of Stretch-Pressure Bioreactor

The stretch bioreactor was validated for its stability in its waveforms. It was able to maintain pressure (Fig. 2a) for the entire duration of the experiment (48 h). The synchrony between the stretch and pressure waveforms was also maintained throughout the course of the experiment.

The results of the dissolved gases test showed that the pH of the pressurized culture media differed from that exposed to atmospheric pressure by −0.0038 ± 0.027. Dissolved oxygen level in the pressurized culture media was 6.16 ± 0.081 mg/L while that in the media exposed to atmospheric condition was 5.03 ± 0.016 mg/L. These results suggest that the high pressure environment within the bioreactor did not cause significant changes to dissolved carbon dioxide and oxygen concentrations.

Tissue Morphology

The three layers of the valve leaflet (fibrosa, ventricularis, and spongiosa) could be seen in the Movat pentachrome stained images (Fig. 3a). The elastin structure of the ventricularis appeared intact, along with the presence of collagen on the fibrosa. This demonstrates that the valve leaflet was not damaged during *ex vivo* experiments.

Changes in the ratio between the fibrosa and spongiosa thicknesses and the ratio between the ventricularis and fibrosa thicknesses are plotted in Fig. 3. The results showed that thickness of the spongiosa and fibrosa increased relative to the ventricularis in the case of pathological stretch (15%) and pressure (140/100 mmHg).

Cell Phenotype Analysis

In general, IHC and immunoblotting results showed that α-SMA expression increased with isolated stretch and decreased when cyclic pressure was applied in combination (Figs. 4b and 5c). α-SMA expression (Fig. 4b) was significantly higher at 15% isolated stretch compared to 10% stretch, which is consistent with our previous report.[1] When cyclic pressure was combined with the cyclic stretch, α-SMA expression decreased as pressure magnitude increased from normal (120/80 mmHg) to pathologic (140/100 mmHg). The

expression of α-SMA in the combined 15% stretch and 140/100 mmHg pressure case was significantly less compared to the isolated 15% stretch case (Fig. 4b).

In contrast, Vimentin expression occurred throughout the leaflet (Fig. 6a). Vimentin seemed to follow the same trends as α-SMA expression. In the isolated 15% stretch case, Vimentin expression was significantly elevated compared to the 10% stretch control and the expression decreased with the increase in magnitude of cyclic pressure. Vimentin expression in the 15% stretch and 140/100 mmHg pressure case was significantly lower compared to the isolated 15% stretch case, following the downward trend (Fig. 6b). The expression in the 10% stretch and 140/100 mmHg case was similar to that of isolated 15% stretch case, and significantly greater compared to the isolated 10% stretch case.

Caldesmon expression was significantly decreased at 15% stretch 140/100 mmHg compared to the normal 10% stretch and 120/80 mmHg case (Figs. 5b and 8). Calponin expression decreased with increasing pressure magnitudes at both levels of stretch (Fig. 7). This trend of Calponin expression resembled that of α-SMA expression, implying a reduction in the contractile phenotype of the valve. This decrease is more apparent in the 15% stretch cases. At 140/100 mmHg pressure, increase in stretch decreased Calponin expression.

DISCUSSION

Loading Conditions

The loading conditions chosen were based on physiological forces experienced by the AV. The cardiac cycle consists of two distinct phases, systole and diastole. The AV leaflets experiences different force combinations in each phase. During systole, the AV is open and it experiences relatively low stretch. During this phase, pressure in the entire aortic root is at its maximum (approximately 120 mmHg in the healthy individual), exposing the entire leaflet to high hydrostatic pressure. During diastole, the AV is closed under transvalvular pressure, and experiences maximum stretch. The aortic surface experiences diastolic aortic pressure (approximately 80 mmHg in the healthy individual), which is lower than systolic aortic pressure, but the ventricular surface experiences very low ventricular pressure (approximately 10–20 mmHg in the healthy individual).

The stretch-pressure bioreactor in the current study exerts stretch and pressure on the valve samples using separate and independent mechanism. Stretch is induced with the stepper motor while pressure is imposed by deflecting the membrane at the top of the chamber. The bioreactor mimics physiological conditions: for 300 ms, the valve leaflets were not stretched, but high systolic aortic pressure was imposed on the leaflets, simulating systole; and for 560 ms, the leaflets were stretched but the relatively lower diastolic aortic pressure was imposed on the leaflets, simulating diastole. The transitions between stretched and relaxed configuration was allowed to occur over 50 ms, simulating the isovolumic relaxation or contraction phases of the cardiac cycle. The only deviation of this configuration from the physiologic mechanical environment was that the ventricular surface of the valve leaflets, which were supposed to experience very low pressures during diastole, were instead exposed to diastolic aortic pressure.

Tissue Morphology

The Movat pentachrome stain showed that the tissue morphology was generally preserved under different conditions, with all three major components, collagen (greenish yellow), GAGs (greenish blue), and elastin (black fibers), visible on the slides. The thickness analysis indicated that the 15% stretch and 140/100 mmHg pressure condition resulted in thickening of the fibrosa and spongiosa layers, which suggest elevated and even pathological remodeling.

Effect of Cyclic Stretch and Pressure on Cellular Phenotype

Our previous studies showed that laminar steady shear stress, static pressure, and cyclic pressure resulted in a reduced level of α-SMA expression in the AV leaflets, while isolated cyclic stretch resulted in an increased expression of α-SMA.[15,26,29,30] It is evident that each of these isolated mechanical stimuli plays a distinct role in regulating the valve phenotype and since the native environment of AV is exposed to a combination of all three mechanical stimuli, it is important to understand the effects of combined forces on the valve phenotype. The current study investigated the effects of combination of cyclic stretch and pressure on the aortic VIC phenotype using a novel *ex vivo* stretch and pressure bioreactor.

As defined by Taylor *et al.*,[28] we allude to three different phenotypes of the VICs. The quiescent or fibroblast phenotype is the one that maintains the *status quo* of the ECM matrix composition and extent. The myofibroblastic phenotype (activated contractile and synthetic) results in the remodeling of the ECM, expresses Vimentin and α-SMA, and may be responsible for valve thickening, leading to disease. The third phenotype is a purely contractile one, more akin to smooth muscle cells. These “smooth muscle-like” cells also are positive for α-SMA as well as Calponin and Caldesmon.

Quiescent VICs express prominent synthetic and secretory organelles, and their role is thought to be the synthesis and stabilization of ECM collagen.[28] Contractile myofibroblasts also remodel the ECM and are characterized by prominent stress fibers associated with α-SMA expression, which is notably absent in quiescent VICs.[23] When the valve is subjected to abnormal hemodynamics, mechanical stress or pathological injury, such as in disease, the quiescent VICs become activated.[24] The exact function of the myofibroblast is still debatable, and it has been suggested they play a role in proliferation and migration,[28] ECM remodeling,[4,24,28] and in altering the stiffness of the valve leaflet in response to mechanical stimuli.[4,18] Further, other authors have also noted that the presence of the activated myofibroblasts in liver, kidney, and arterial injuries are associated with elevated apoptosis.[6] The same may occur in the AV, which may be relevant to calcification since apoptosis is known to be involved in valve calcification.[12] It is noted that the results presented pertain to the acute phenotypic changes of the VICs and may not necessarily indicate eventual disease. Indeed, these may be compensatory responses to the acute changes in the mechanical environment. Further studies are necessary to investigate if a causal relation between the phenotype changes and the development of a diseased state exists.

In the present study, we demonstrate how cyclic stretch and pressure can influence this phenotypic modulation, alternating between quiescent and activated states, even within a

short duration of 48 h. It was observed that increased pressure decreased α-SMA expression, while increased stretch increased α-SMA expression, which agrees with our previous studies.[1,31] Our results indicate that the response of the AV leaflets to the combination of cyclic stretch and pressure may be a direct superposition of the responses to cyclic stretch alone and the response to pressure alone. The opposing effects of pressure and stretch on α-SMA therefore suggest that the combined normal physiological hemodynamic forces act to maintain the quiescent phenotype and prevent expression of the activated contractile phenotype.

Further, it appears that tensile stretch and pressure on the AV leaflet act to oppose each other. The application of cyclic pressure suppressed the increase in α-SMA expression caused by elevated stretch. At 140/100 mmHg pressure, the increase in stretch appeared to have no effect on α-SMA expression, while without pressure, increase in stretch significantly increased α-SMA expression. On the other hand, the decrease in α-SMA expression brought about by elevated pressure appeared more significant at 15% stretch compared to at 10% stretch. Comparing the physiologically normal condition of 10% stretch and 120/80 mmHg pressure and the hypertensive condition of 15% stretch and 140/100 mmHg pressure, however, we observed that there was a decrease in α-SMA expression (significance was observed in the immunoblotting results). Take as a whole, these results suggest that excessive pressure could have suppressed the contractile phenotype and induced the differentiation into an activated synthetic phenotype. This result agrees well with observed increased leaflet thickness in the hypertensive, 15% stretch 140/100 mmHg condition. Further, we speculate that any reduction in the quiescent phenotype may indicate a lack of protective response against additional deformational trauma, and may hold implications regarding the association of hypertension to AV diseases.[22] Further investigation will be required to verify this.

Vimentin, another myofibroblast marker, is the sole intermediate filament protein of endothelial cells covering the inner surface of all blood vessels, chambers, and valves of the heart.[8] Vimentin filaments are present in the semi-elastic intracellular scaffold, and have been hypothesized to help cells maintain their overall cellular morphology and to protect them against mechanical injury from blood flow, wall extension, and pressure.[26] The Vimentin results showed that it was significantly upregulated when isolated cyclic stretch was increased from normal (10%) to pathologic (15%) levels, except for the 140/100 mmHg pressure condition, suggesting a valvular response to the increased tensile forces may be the production of Vimentin to withstand the increased force and prevent tissue damage. At the 15% stretch and 140/100 mmHg pressure condition, however, Vimentin expression was very low, again suggesting that a protective mechanism may have not engaged with hypertension. Interestingly, Vimentin expression was greatly increased from no pressure to pathological pressure (140/100 mmHg) in the normal stretch (10%) case, this increase could be the result of the imbalance of a normal tensile force and a pathological pressure force.

Activation of non-smooth muscle-like cells such as fibroblasts has been shown to stimulate rapid polymerization of actin from monomeric Globular (G) Actin to Filamentous (F) Actin form.[17] Caldesmon is required for the bundling activity of actin.[9] Calponin acts as a nucleator in Actin polymerization or inhibits the depolymerization.[13] The expression trends

of Calponin resembled that of α-SMA, where increase in pressure decreased the expression levels of Calponin. Further, immunoblotting results showed that Caldesmon expressions was at the lowest at the 15% stretch 140/100 mmHg pressure condition. This correlated with the low expression levels of α-SMA and Vimentin as well. This may indicate that Calponin and Caldesmon play a role in the maintenance of valvular phenotype by influencing the kinetics of Actin polymerization.

The results suggest that the expression of α-SMA, Vimentin, Caldesmon, and Calponin are sensitive to differing magnitudes of pressure and stretch. Our results agreed with observations by other authors that VICs have high adaptability to changes in their environment.[4,28] In our study, trends in the protein expressions were observable despite the short duration of study of 48 h, suggesting that the AV adapts to altered mechanical environment rapidly, allowing it to retain normal biological functions.

LIMITATIONS

A limitation of this study was that markers specific for fibroblasts were not analyzed, which is another phenotype of the VIC.[28] The analysis was especially challenging as there were no commercially available antibodies specific for the porcine fibroblast. The valves were stretched under uniaxial conditions rather than biaxial conditions, and their ventricular surface were exposed to aortic pressure during diastole. These were non-physiologic, but were inevitable due to the bioreactor experimental setup. Future studies will focus on analyses at the gene level to discern if any fibroblast-specific markers were upregulated by cyclic stretch and pulsatile pressure.

CONCLUSION

This study demonstrated that a combination of cyclic stretch in the circumferential direction and cyclic pressure modulated the expression of various myofibroblast markers such as α-SMA, Vimentin, and Calponin in a magnitude-dependent manner, suggesting downregulation of contractile phenotype under hypertensive conditions. Further, we speculate that the hypertensive mechanical condition may modulate protective mechanisms in the AV tissues, which may play a role in the correlation between hypertension and AV diseases.

Acknowledgments

National Science Foundation through the Engineering Research Center program at Georgia Tech/Emory Center for the Engineering of Living Tissues under award EEC-9731643. Holifield Farms for providing porcine hearts for the research. Patrick Thayer was supported by the President's Undergraduate Research Award (PURA).

References

1. Balachandran K, et al. An *ex vivo* study of the biological properties of porcine aortic valves in response to circumferential cyclic stretch. Ann Biomed Eng. 2006; 34(11):1655–1665.
2. Balachandran K, et al. Elevated cyclic stretch alters matrix remodeling in aortic valve cusps—implications for degenerative aortic valve disease? Am J Physiol Heart Circ Physiol. 2009; 296(3):H756–H764. [PubMed: 19151254]

3. Balachandran K, et al. Elevated cyclic stretch induces aortic valve calcification in a bone morphogenic protein-dependent manner. Am J Pathol. 2010; 177(1):49–57. [PubMed: 20489151]
4. Chester AH, Taylor PM. Molecular and functional characteristics of heart-valve interstitial cells. Philos Trans R Soc Lond B Biol Sci. 2007; 362(1484):1437–1443. [PubMed: 17569642]
5. Della Rocca F, et al. Cell composition of the human pulmonary valve: a comparative study with the aortic valve-the VESALIO* project. Ann Thorac Surg. 2000; 70(5):1594–1600. [PubMed: 11093493]
6. Desmouliere A, et al. Apoptosis during wound healing, fibrocontractive diseases and vascular wall injury. Int J Biochem Cell Biol. 1997; 29(1):19–30. [PubMed: 9076938]
7. El-Mezgueldi, M Calponin. Apoptosis during wound healing, fibrocontractive diseases and vascular wall injury. Int J Biochem Cell Biol. 1996; 28(11):1185–1189. [PubMed: 9022277]
8. Franke WW, et al. Intermediate sized filaments of human endothelial cells. J Cell Biol. 1979; 81(3): 570–580. [PubMed: 379021]
9. Galqzkiewicz B, et al. Polymerization of G-actin by caldesmon. FEBS Lett. 1985; 184(1):144–149. [PubMed: 2985442]
10. Hossain MM, et al. h2-Calponin is regulated by mechanical tension and modifies the function of actin cytoskeleton. J Biol Chem. 2005; 280(51):42442–42453. [PubMed: 16236705]
11. Ingber D. Mechanobiology and diseases of mechano-transduction. Ann Med. 2003; 35(8):564–577. [PubMed: 14708967]
12. Jian B, et al. Progression of aortic valve stenosis: TGF-betal is present in calcified aortic valve cusps and promotes aortic valve interstitial cell calcification via apoptosis. Ann Thorac Surg. 2003; 75(2):457–465. discussion 465–466. [PubMed: 12607654]
13. Kake T, et al. Calponin induces actin polymerization at low ionic strength and inhibits depolymerization of actin filaments. Biochem J. 1995; 312:587–592. [PubMed: 8526874]
14. Konduri S, et al. Normal physiological conditions maintain the biological characteristics of porcine aortic heart valves: an *ex vivo* organ culture study. Ann Biomed Eng. 2005; 33(9):1158–1166. [PubMed: 16133923]
15. Liu AC V, Joag R, Gotlieb AI. The emerging role of valve interstitial cell phenotypes in regulating heart valve pathobiology. Am J Pathol. 2007; 171(5):1407–1418. [PubMed: 17823281]
16. Marston SB, Redwood CS. The molecular anatomy of caldesmon. Biochem J. 1991; 279(1):1–16. [PubMed: 1930128]
17. Mehta D, Gunst SJ. Actin polymerization stimulated by contractile activation regulates force development in canine tracheal smooth muscle. J Physiol Lond. 1999; 519(3):829–840. [PubMed: 10457094]
18. Merryman WD, et al. Synergistic effects of cyclic tension and transforming growth factor-beta1 on the aortic valve myofibroblast. Cardiovasc Pathol. 2007; 16(5):268–276. [PubMed: 17868877]
19. Mohler ER III. Mechanisms of aortic valve calcification. Am J Cardiol. 2004; 94(11):1396–1402. [PubMed: 15566910]
20. North AJ, et al. Calponin is localised in both the contractile apparatus and the cytoskeleton of smooth muscle cells. J Cell Sci. 1994; 107(3):437–144. [PubMed: 8006064]
21. Philippe S, et al. Design of an *ex vivo* culture system to investigate the effects of shear stress on cardiovascular tissue. J Biomech Eng. 2008; 130(3):035001. [PubMed: 18532871]
22. Rabkin SW. The association of hypertension and aortic valve sclerosis. Blood Press. 2005; 14(5): 264–272. [PubMed: 16257871]
23. Rabkin E, et al. Activated interstitial myofibroblasts express catabolic enzymes and mediate matrix remodeling in myxomatous heart valves. Circulation. 2001; 104(21):2525–2532. [PubMed: 11714645]
24. Rabkin-Aikawa E, et al. Dynamic and reversible changes of interstitial cell phenotype during remodeling of cardiac valves. J Heart Valve Dis. 2004; 13(5):841–847. [PubMed: 15473488]
25. Schneider PJ, Deck JD. Tissue and cell renewal in the natural aortic valve of rats: an autoradiographic study. Cardiovasc Res. 1981; 15(4):181–189. [PubMed: 7273050]
26. Schnittler HJ, Schmandra T, Drenckhahn D. Correlation of endothelial vimentin content with hemodynamic parameters. Histochem Cell Biol. 1998; 110(2):161–167. [PubMed: 9720988]

27. Sucosky P, et al. Altered shear stress stimulates upregulation of endothelial VCAM-1 and ICAM-1 in a BMP-4-and TGF-beta1-dependent pathway. Arterioscler Thromb Vasc Biol. 2009; 29(2):254–260. [PubMed: 19023092]
28. Taylor PM, et al. The cardiac valve interstitial cell. Int J Biochem Cell Biol. 2003; 35(2):113–118. [PubMed: 12479860]
29. Wang N, Stamenovic D. Mechanics of vimentin intermediate filaments. J Muscle Res Cell Motil. 2002; 23(5):535–540. [PubMed: 12785103]
30. Xing Y, et al. Effects of constant static pressure on the biological properties of porcine aortic valve leaflets. Ann Biomed Eng. 2004; 32(4):555–562. [PubMed: 15117029]
31. Xing Y, et al. Cyclic pressure affects the biological properties of porcine aortic valve leaflets in a magnitude and frequency dependent manner. Ann Biomed Eng. 2004; 32(11):1461–1470. [PubMed: 15636107]

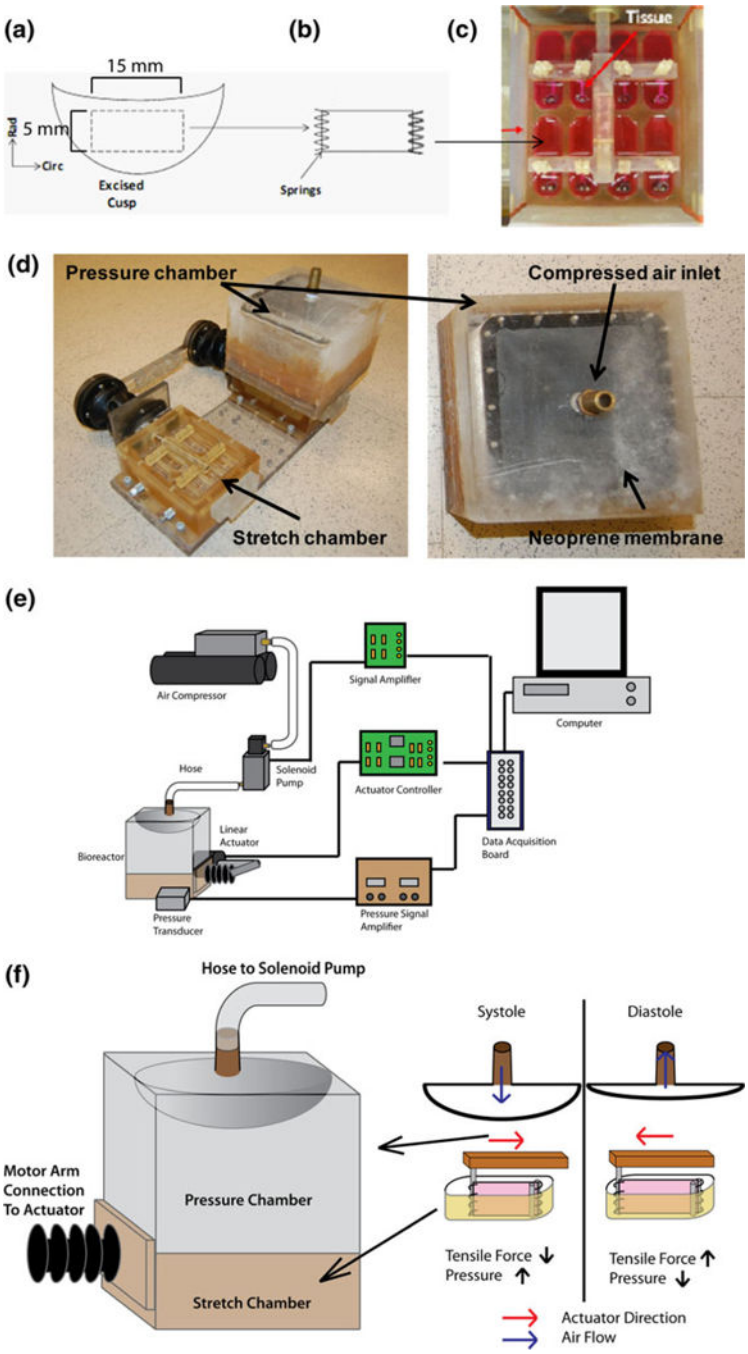

FIGURE 1.

(a) 15 by 5 mm section excised from AV leaflet, (b) threaded with springs on the 5 mm end, and (c) inserted into bioreactor tissue chamber. (d) Photograph depicting the design of the stretch-pressure bioreactor. (e) Schematic depicting the experimental setup and (f) mechanisms of stretch and pressure application in the bioreactor.

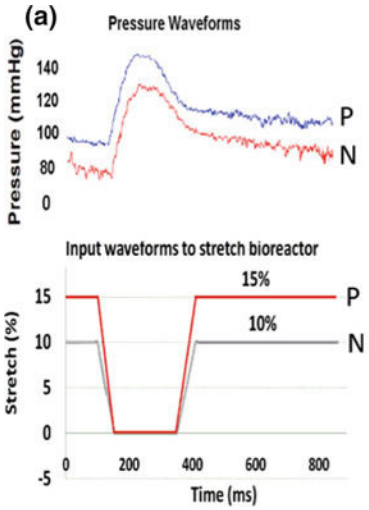

(b)

Conditions	
10% Stretch (N)	-
10% Stretch (N)	120/80 mmHg (N)
10% Stretch (N)	140/100 mmHg (P)
15% Stretch (P)	-
15% Stretch (P)	120/80 mmHg (N)
15% Stretch (P)	140/100 mmHg (P)

FIGURE 2.

(a) Output waveforms for pressure and input waveforms for stretch shown over one cardiac cycle (N: normal and P: pathologic). (b) Mechanical treatment conditions tested in this study.

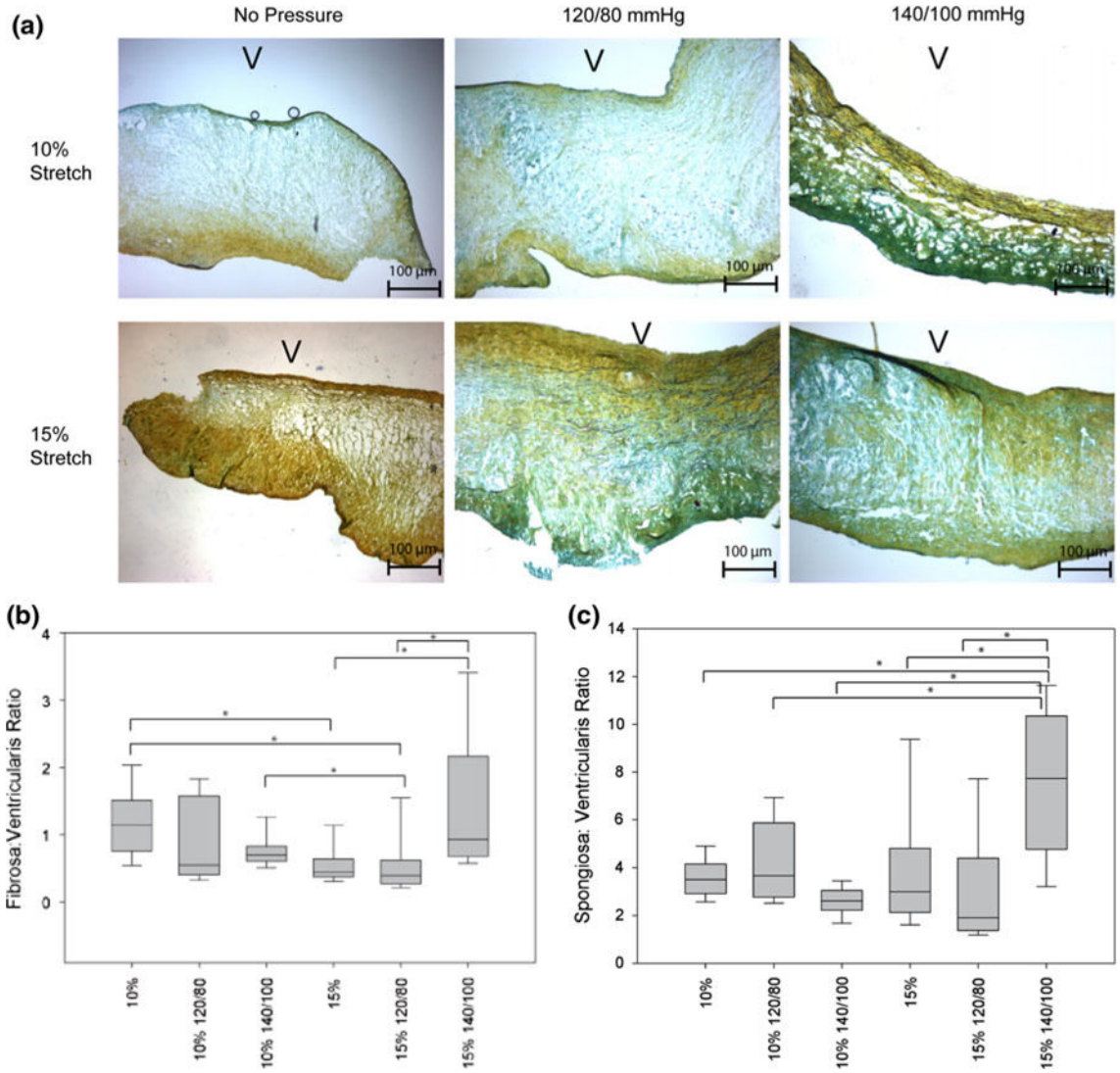

FIGURE 3.

(a) Movat pentachrome stain of AV leaflets at various stretch and pressure conditions (V: ventricularis). (b) The ratio between the fibrosa and the ventricularis and the spongiosa and the ventricularis is shown here (*p< 0.05).

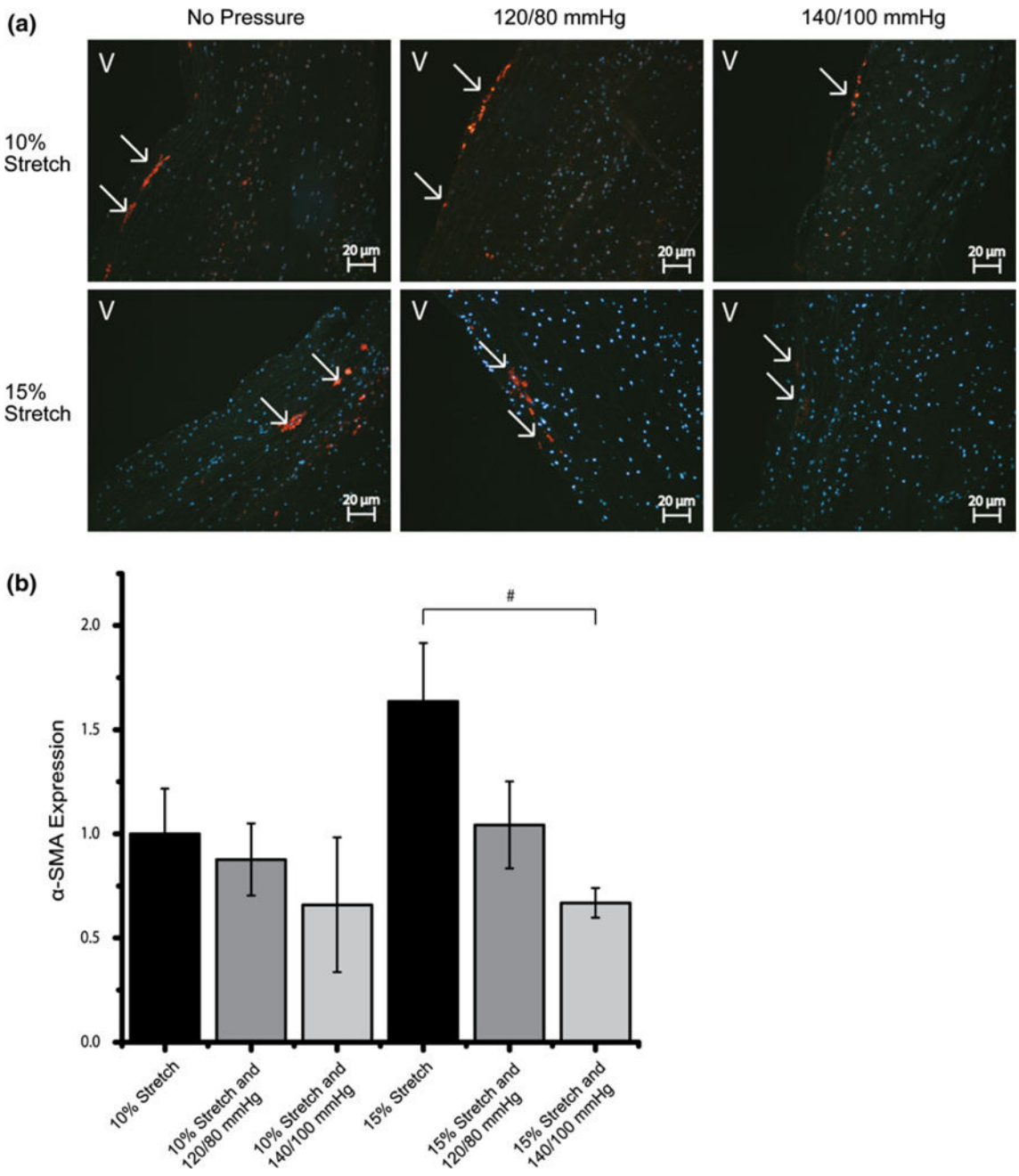

FIGURE 4.

IHC images and expression levels of α-SMA expression normalized by the mean expression level in the isolated 10% stretch condition ($^{\#}p < 0.10$). α-SMA was stained red and cell nuclei were counterstained blue (V: ventricularis).

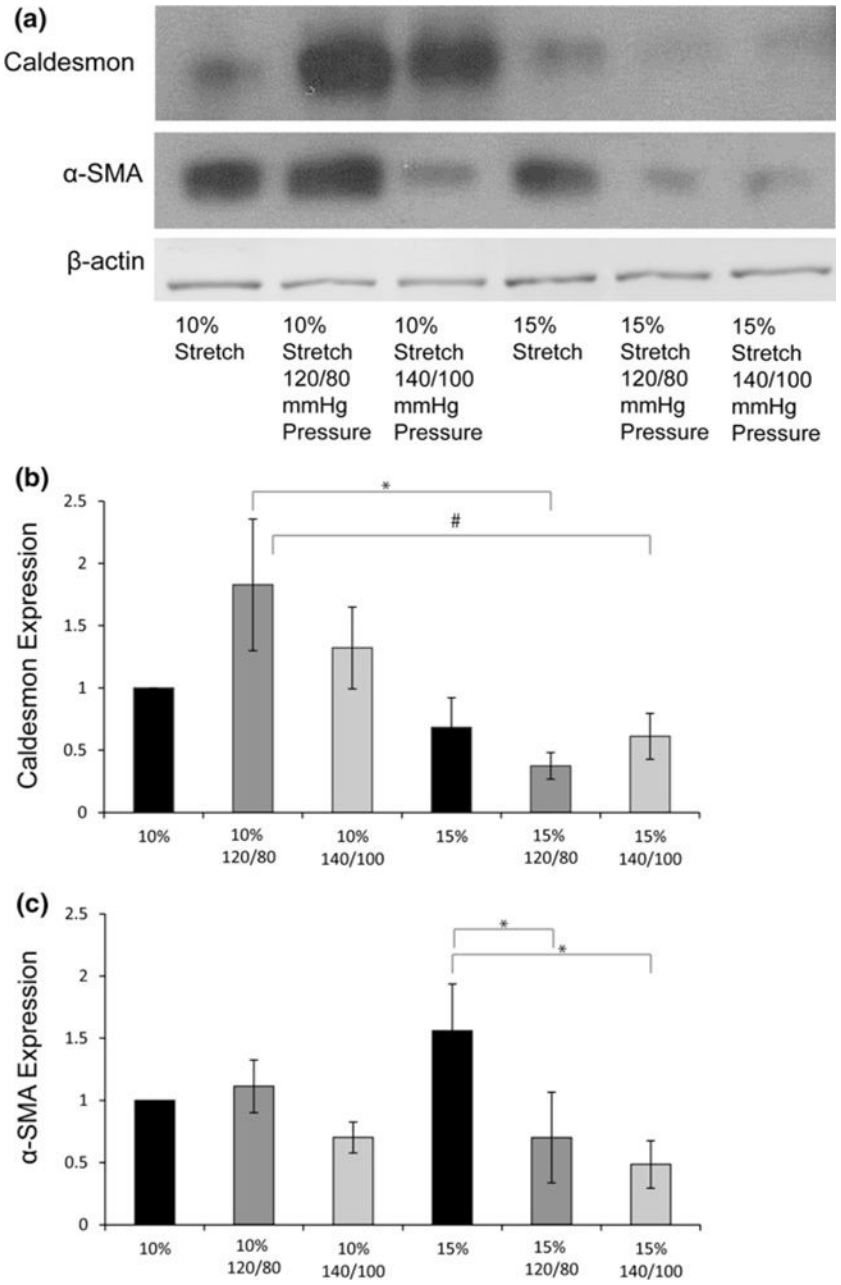

FIGURE 5.

(a) Immunoblot bands for Caldesmon, α-SMA, and β-actin (b, c, d) expression of the various proteins normalized to β-actin and then the 10% stretch case ($^{*}p < 0.05$, $^{\#}p < 0.10$).

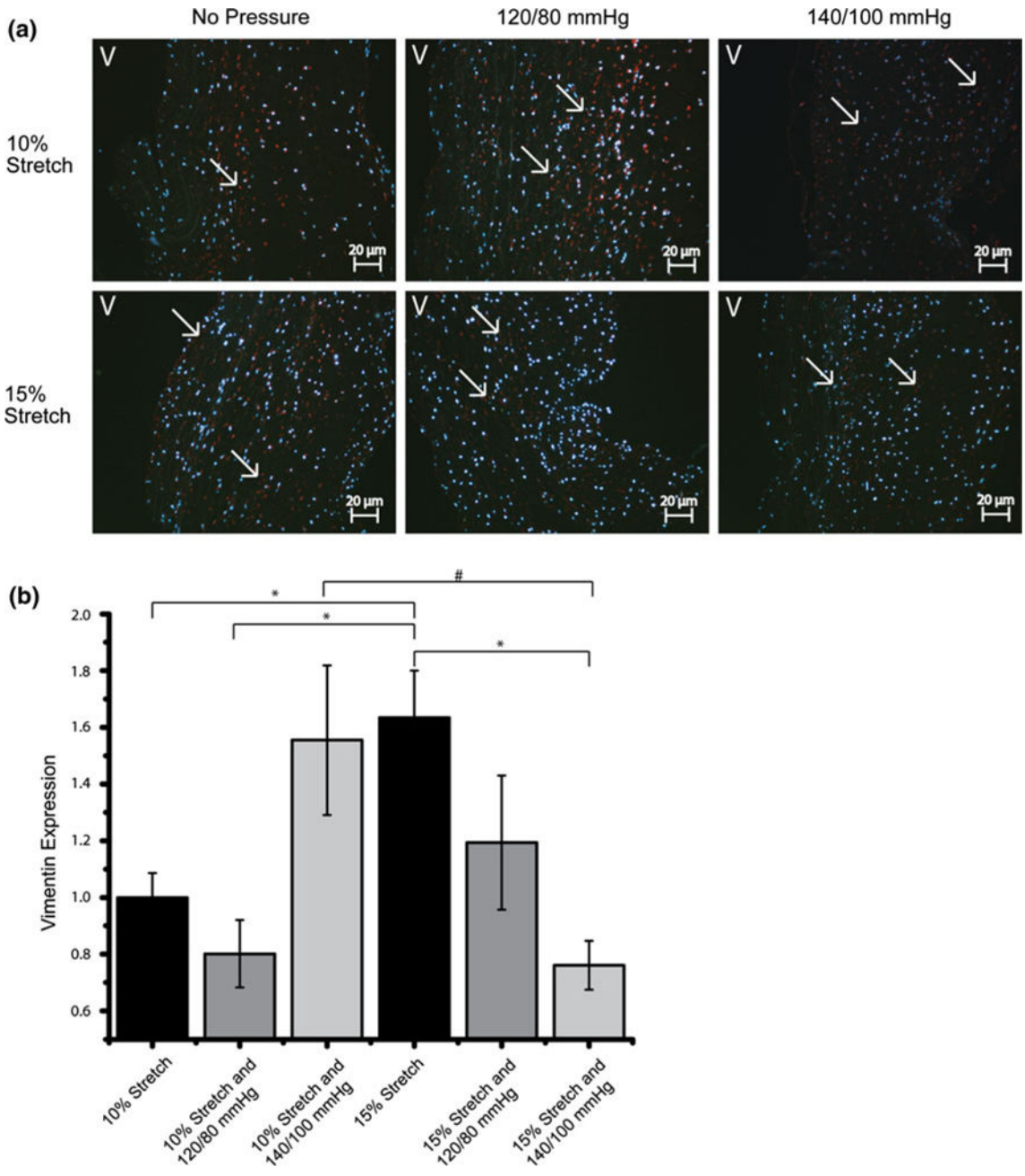

FIGURE 6.

IHC images and expression levels of Vimentin expression normalized by the mean expression level in the isolated 10% stretch condition (*$p < 0.05$, $^{\#}p < 0.10$). Vimentin was stained red and cell nuclei were counterstained blue (V: ventricularis).

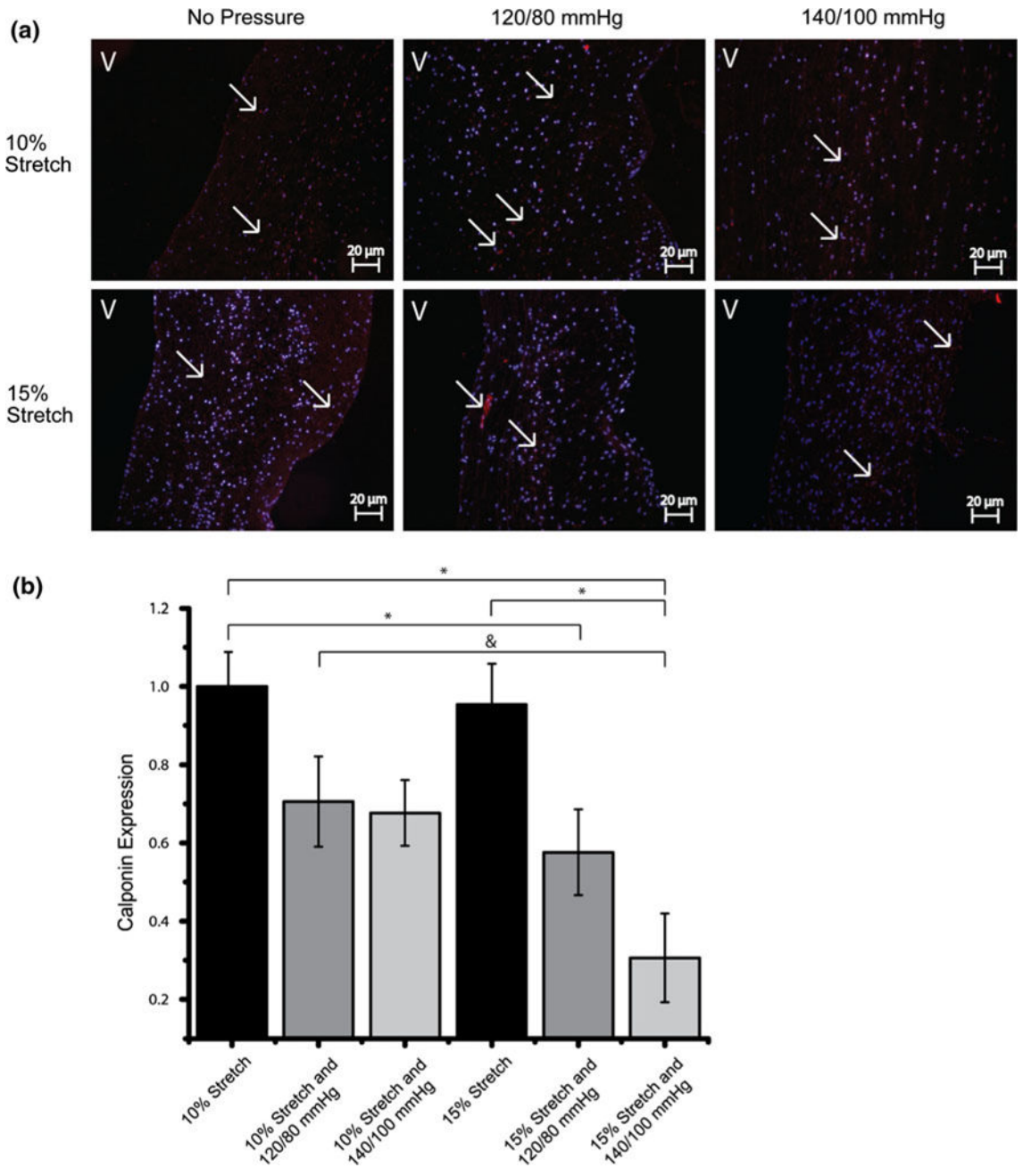

FIGURE 7.

IHC images and expression levels of Calponin expression normalized by the mean expression level in the isolated 10% stretch condition (*p< 0.05). Significance between the normal condition (10% and 120/80 mmHg) and the hypertensive condition (15% and 140/100 mmHg) is marked with a "&" (p< 0.05). Calponin was stained red and cell nuclei were counterstained blue (V: ventricularis).

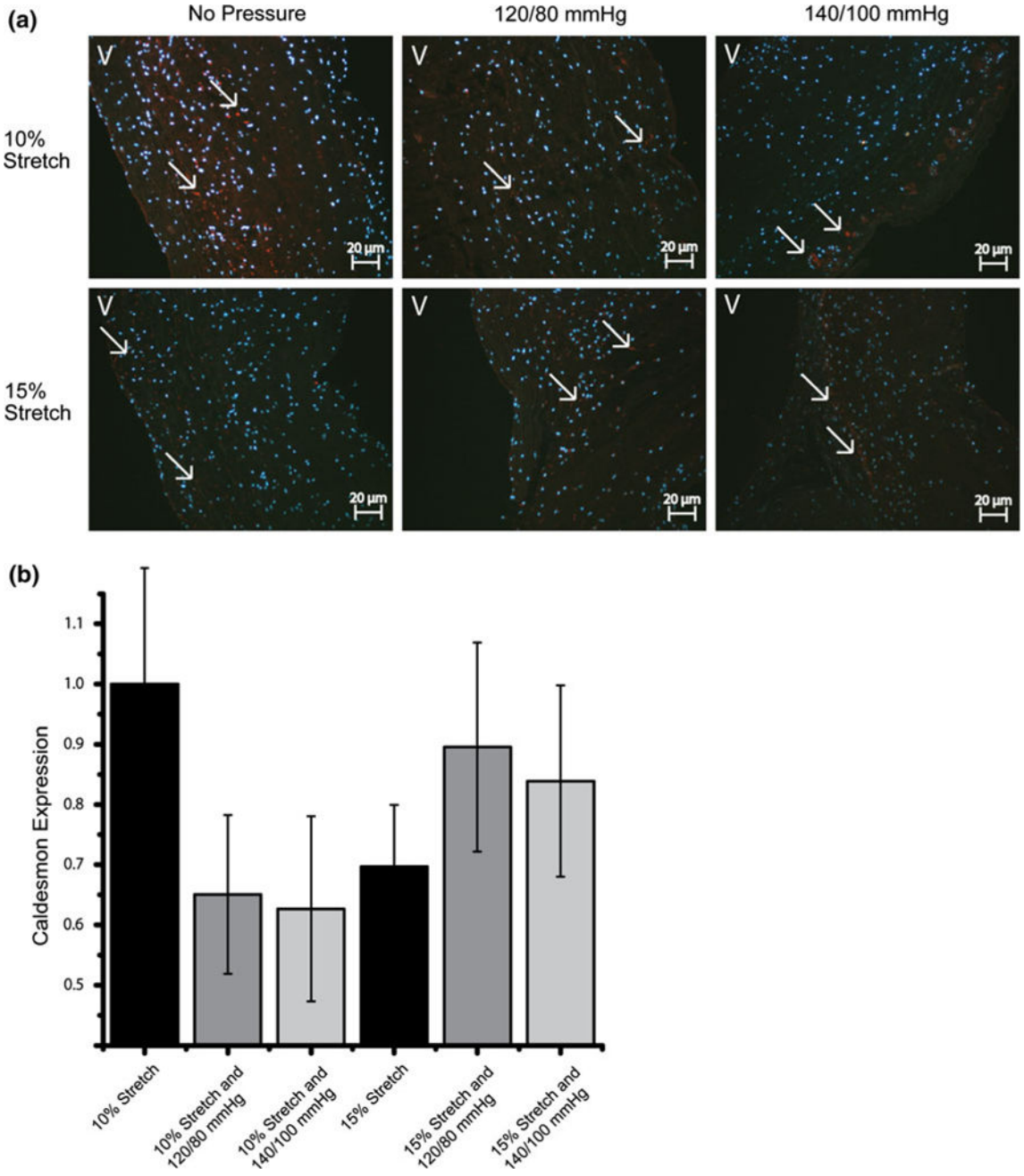

FIGURE 8.

IHC images and expression levels of Caldesmon expression normalized by the mean expression level in the isolated 10% stretch condition (*$p < 0.05$). Caldesmon was stained red and cell nuclei were counterstained blue (V: ventricularis).